Journal of Image Processing and Intelligent Remote Sensing
ISSN 2815-0953
Vol: 03, No. 03, April-May 2023
http://journal.hmjournals.com/index.php/JIPIRS
DOI: https://doi.org/10.55529/jipirs.33.1.8

A New Filter Design Built Into CMOS Image Sensor

Zuhair Shakor Mahmmod[1]*, Ali Nasret Najdet[2], Abbas B. Noori[3]

[1,2,3]Department of Electronic, Northern Technical University , Mosul, Iraq*

Corresponding Email: [1]zuherkazanci@ntu.edu.iq*

Received: 04 December 2022 **Accepted:** 28 February 2023 **Published:** 03 April 2023

Abstract: ***dry etch and Electron beam lithography were used to directly integrate plasmonic color filters onto the top surface of a complementary metal oxide semiconductor (CMOS. The filters have a spectral range of 3.5 × 8 microns. After measuring the photocurrent, it was found that the 150×150-pixel plasmonic CIS was sensitive to all colors in the visible spectrum. The filters were made using a straightforward method that only required a single lithographic procedure. This is in contrast to the standard multi-stage processing required when working with dyedoped polymers. It is possible to fabricate these plasmonic components on a metal layer near to the photodiodes since they are intrinsically compatible with a typical CMOS process. Future low-cost, low-cross-talk, high-functionality advanced CIS may be possible with the help of such plasmonic components.***

Keywords: Subwavelength Structures, Surface Plasmons, CMOS Image Sensors, Colour Filters.

1. INTRODUCTION

Solid-state digital imaging is dominated by image sensors, which are made from CMOS. Complementary metal oxide semiconductors image sensor has several advantages, such as low power depreciation, compatibility with traditional CMOS, implementation of integrated functionality, and the low voltage operation. The last ten years have seen a dramatic rise in CIS performance thanks to the shrinking of feature sizes in complementary metal oxide semiconductors technology. Nevertheless, traditional Color cross-talk and other performance issues plague CIS dye-doped polymer color filters., when pixel size is reduced to the sub-2 µm range. In addition, the fabrication of these filters requires a series of stages that must be completed in order. For CIS to have consistent growth in usefulness, it must be commercially viable even when new applications are developed [1, 2]. It is preferable to develop other methods of producing color filters for CIS because to the growing issues of cross-talk and the high cost of fabrication utilizing the dye-doped polymer approach. Although other methods have been explored, such as silicon subwavelength gratings, multiple Fabry-Pérot and

Copyright The Author(s) 2023.This is an Open Access Article distributed under the CC BY license. (http://creativecommons.org/licenses/by/4.0/)

Journal of Image Processing and Intelligent Remote Sensing
ISSN 2815-0953
Vol: 03, No. 03, April-May 2023
http://journal.hmjournals.com/index.php/JIPIRS
DOI: https://doi.org/10.55529/jipirs.33.1.8

multilayer photonic crystal color filterscavities made from metal mirrors, their low performance and difficult construction mean they have limited practical applicability. Thin metal films patterned with nanostructures may also be used for surface plasmon resonance (SPR), making them a promising material with which to create filters. Depending on the nanostructures of the metal sheet, the incident light links with the surface plasmon in a certain manner[3,4,5]. By altering the nanostructures, the resonant wavelength may be tuned, allowing the desired light filtration to be achieved. As a result of this method, it may be possible to create all the necessary color filters in a single layer. By incorporating plasmonic color filters in the metal layers below the CMOS photodiodes, we can cut down on both costs and color cross-talk. SPR's adaptability also means it has the potential to bring advanced optical capabilities to the CIS. A number of studies have shown positive outcomes when using plasmonic filters, but to the best of our knowledge, no studies have described the use of a CIS that included plasmonic elements. With the help of thorough numerical simulations and early experimental findings. demonstrated the possible use of plasmonic filters. To block out infrared light, incorporated metal gratings into a CIS to create a filter with a passband in the visible. SPR was found to boost photocurrent in a CMOS detector with a C-shaped nanoaperture. In the recent past, plasmonic color filters for use in large area single-pixel CMOS photodetectors have been developed. were shown to function in the visible spectrum. Electron beam lithography (EBL) was used to manufacture the aluminum nanostructures that made up the filter on the surface of the plasmonic CIS (pCIS), which coated an area of the photodiode that was around 1 mm^2[6,7,8].

We show a 150×150-pixel pCIS with pixel sizes of 5×9.5 µm. Specifically, the AMS 0.4 µm process was used to fabricate the CIS in a microelectronics foundry. When it came time to include plasmonic components onto the CIS, we did the processing at the tail end of the production line in our own labs. These filters were created using the CIS and a glass calibration sample for spectral comparison. Both the glass samples and the pCIS were characterized by measuring the integrated photocurrent at the photodiodes in a microscope spectrophotometer. The 150×150-pixel plasmonic CIS was very sensitive to colors throughout the visible spectrum [9,10,11].

Optical Glass with Plasmonic Color Filters

examined a periodic λ_{max} represent of subwavelength hole array in a silver sheet, they found a number of unexpected optical properties, including increased transmission of The holes let some light through, while the activated SPR acts as a filter for certain wavelengths. By observing the normal incidence transmission spectra of a triangular lattice with holes spaced at subwavelength intervals, the peak location, λ_{max}, may be approximatively determined as

$$\lambda_{max} = \frac{a}{\sqrt{\frac{4}{3}(i^2 + ij + j^2)}} \sqrt{\frac{\varepsilon_m \varepsilon_d}{\varepsilon_m + \varepsilon_d}} \qquad (1)$$

The orders of the array are determined by the numbers i and j, where an is the period of the array, ε_d and ε_m represent dielectric material and the dielectric constants of the metal in contact with the metal, iand j are both positive[12,13].

Copyright The Author(s) 2023.This is an Open Access Article distributed under the CC BY license. (http://creativecommons.org/licenses/by/4.0/)

Journal of Image Processing and Intelligent Remote Sensing
ISSN 2815-0953
Vol: 03, No. 03, April-May 2023
http://journal.hmjournals.com/index.php/JIPIRS
DOI: https://doi.org/10.55529/jipirs.33.1.8

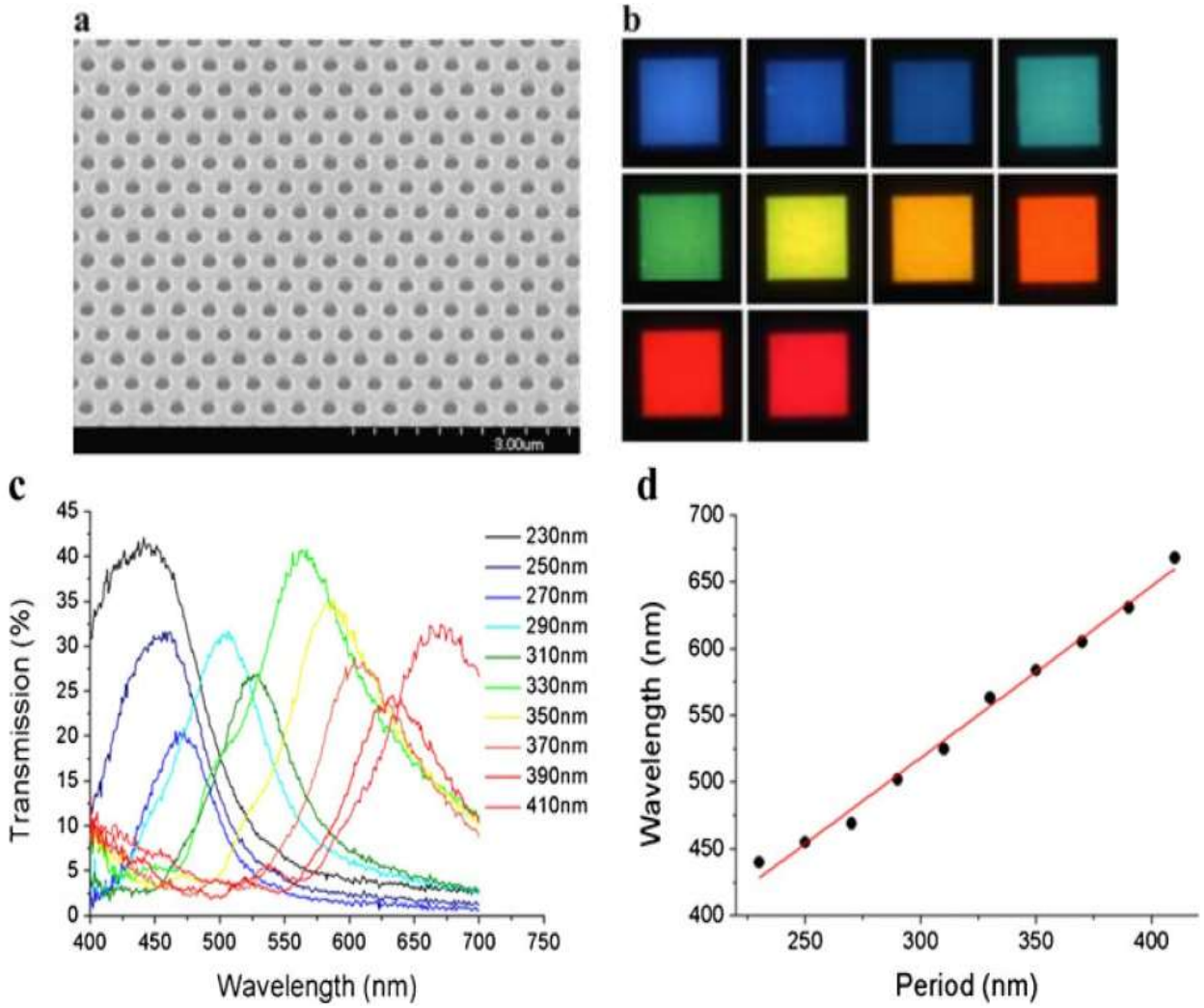
As an alternative to more expensive noble metals like gold and silver, aluminium was chosen in this study since it is often used in CMOS processes. Plasmonic filters were first created on a glass substrate to evaluate the designs of these filters. To begin making these filters, an aluminum layer 160 nm in thickness was evaporated onto a glass substrate using an electron beam evaporator (Plassys MEB 400S).Once It was created using a ZEP520A electron beam resist that had been twist onto the irradiated and sample using a VB6 electron beam system. When the pattern was developed using o-xylene, it was transferred using a SiH4 dry etch in a Plasmalab System 100. To improve transmission, a plasma-enhanced chemical vapour-deposited, top SiO_2 layer of 200 nm was used to boost SPR coupling on both sides of the metal film. FIGURE 1a shows a scanning electron micrograph of an aluminum substrate with a periodic array of holes 410 nm in size. An Olympus AX70 microscope equipped with a broadband halogen light was used to study color pictures of plasmonic filters with varying nanostructures on the same material. Squares of color, each 70×70 µm in size, are made up of holes in a triangular lattice of aluminum with varying period (see Figure 1b). We took the spectra using a TFProbe MSP300 spectrophotometer, a microscope-mounted spectrometer capable of taking readings from a spot as small as 10×10 µm. A typical beam of unpolarized light from a halogen lamp was fired onto the sample's back. In Fig. 1c, we see the sample's transmission spectra in the visible range (400-700 nm), where transmittances vary from 20 to 40 percent and full width at half maximum values range from80 to 135 nm. As a result of the non-zero imaginary component of the permittivity, loss processes like as absorption occur inside the metal itself, re-radiation, and reflection,. According to Fig. 1d, The length of time that holes were present in the metal layer. causes a linear rise in the λ_max at which transmission through each filter reaches its maximum., as anticipated by Eq. (1). This proves that a whole set of color filters can be manufactured with high reliability using only one lithographic process[17,20].

A CIS with Built-in Plasmonic Color Filters

We installed the plasmonic filters onto a CIS to investigate their functionality in digital photography. In this study, a CIS with a 150×150-pixel array have been employed. The pixel size is 10×10 µm, as shown in Fig. 2a, and each pixel has a 3.5 × 8 µm photodiode, with a 0.7 µm inter-photodiode gap between certain pixels. As can be seen in Fig. 2b, the top metal layer in the AMS 0.45 µm process causes the pixels' topography to have a vertical step of 1.1 µm between circuit sections and the photodiode inside each pixel. Fabrication methods different from those utilized to create plasmonic filters on glass are required. So as to increase light flow through the CIS's built-in color filters. The150 kV EBL system with a backscatter detector has trouble registering precisely to the pixels on CMOS chips because of the aluminum they contain. As a result, we deposit gold electrons in about Figure 1 Comparison of glass-fabricated plasmonic color filters of varying strengths. A- scanning electron microscope picture of a plasmonic color filter made from aluminum b- featuring a periodic grid of holes measuring 410 nm in size. transmission mode microscopy images captured using a variety of plasmonic color filters and white light. Transmittance spectra for the shown filters in (c). d- the peak wavelengths of transmission through each plasmonic nanostructure versus their periods

Copyright The Author(s) 2023.This is an Open Access Article distributed under the CC BY license. (http://creativecommons.org/licenses/by/4.0/)

Journal of Image Processing and Intelligent Remote Sensing
ISSN 2815-0953
Vol: 03, No. 03, April-May 2023
http://journal.hmjournals.com/index.php/JIPIRS
DOI: https://doi.org/10.55529/jipirs.33.1.8



conventional lift-off procedure around the CIS beam markers. The fictitious pattern is then written to the pixel array through a registration EBL step, we compare the positions of our gold markers to the pixel array and calculate the positioning error. The final pattern is then written using this information in a third EBL step onto an evaporated 160-nm aluminium film placed directly on the photodiode array. If this method were included into the foundry's production process, just a single lithography step would be necessary. A last-minute masking and etching Figure 2.as seen via a microscope. It's an unprocessed AFM image of pixel topography. The photodiode pixel array with manufactured plasmonic color filters, as shown in a microscope picture. d A scanning electron micrograph showing a CIS with plasmonic color filters attached. A magnified view of a 230-nanometer-long period filter is shown in the inset.

Copyright The Author(s) 2023.This is an Open Access Article distributed under the CC BY license. (http://creativecommons.org/licenses/by/4.0/)

Journal of Image Processing and Intelligent Remote Sensing
ISSN 2815-0953
Vol: 03, No. 03, April-May 2023
http://journal.hmjournals.com/index.php/JIPIRS
DOI: https://doi.org/10.55529/jipirs.33.1.8

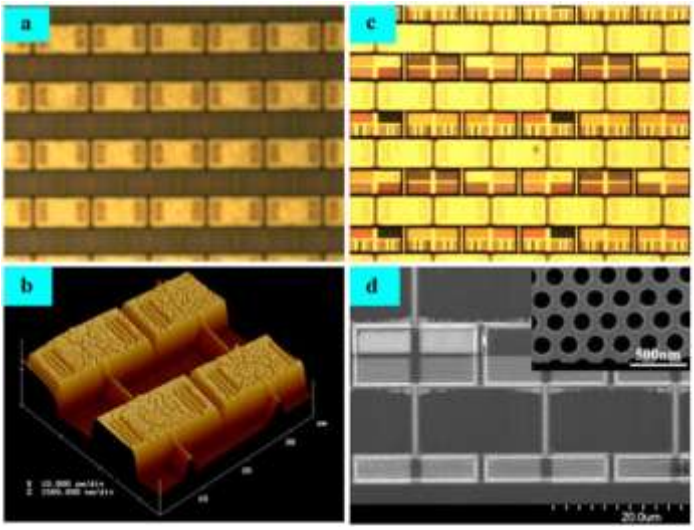
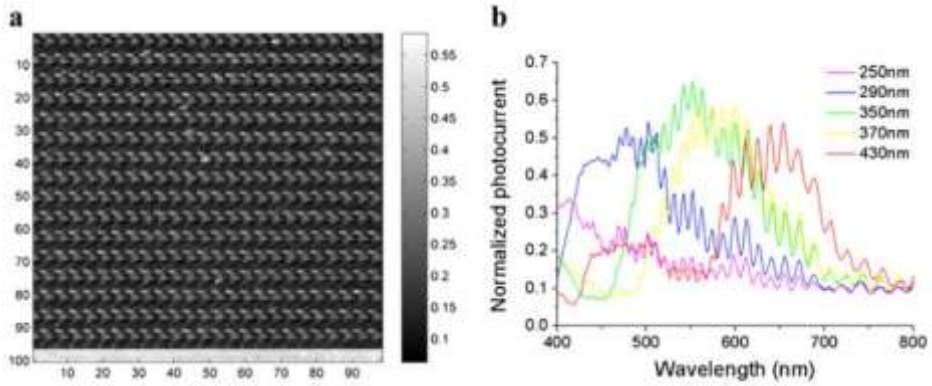


Figure 3. a- the overall distribution of photocurrent over the 150×150 photodiode array. b- the Employing a variety of plasmonic color filters, photocurrents of photodiodes were adjusted before being measured.



reopening windows over the IC bond pads was a necessary step. The treated pixels, which consisted of a sequence of variable plasmonic components repeated throughout the photodiode pixel array, are seen in Fig. 2c, which is a microscope view of the processed pixels. Differently designed nanostructures produce varied spectral phase reflections, each of which can be seen in this reflection picture. Reference pixels, for which the aluminum coating over the photodiodes has been completely removed, appear as black rectangles. In Fig. 2d, we observe a SEM picture of the pixels equipped with plasmonic filters, and we can see that the plasmonic structure is well aligned to each pixel. A whole array with a period of 230 nm is seen in the inset of Fig. 2d. These filters allow a deep blue light to pass through.

Tests were performed on the pixel array by shining light in the range of 500 to 900 nm onto it from a tungsten lamp via a monochromator. Although the center wavelength was adjusted in 2-nm steps, the slits employed inside the monochromator were selected to restrict the range of wavelengths to 5 nm for each experiment. Each pixel's response was measured at its respective center wavelength with the use of a data gathering equipment, namely a National Instruments

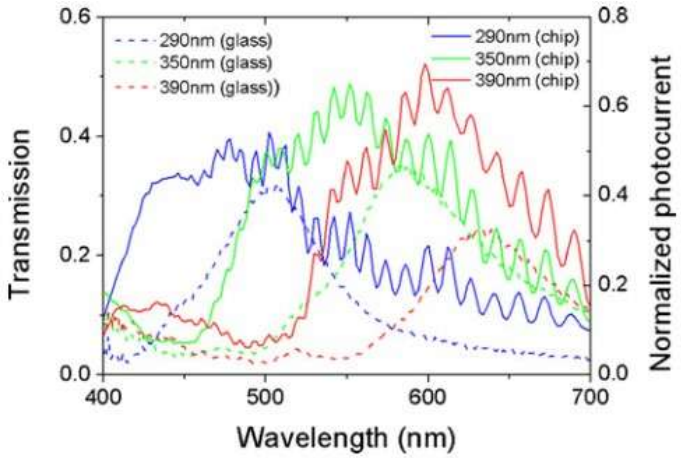
Copyright The Author(s) 2023.This is an Open Access Article distributed under the CC BY license. (http://creativecommons.org/licenses/by/4.0/)

Journal of Image Processing and Intelligent Remote Sensing
ISSN 2815-0953
Vol: 03, No. 03, April-May 2023
http://journal.hmjournals.com/index.php/JIPIRS
DOI: https://doi.org/10.55529/jipirs.33.1.8

USB-6218. After integrating the data for 125 ms, we were able to calculate the response of each pixel and apply the necessary corrections for fixed pattern noise. Also, the response at each center wavelength was adjusted by subtracting the pixel's integrated response after 125 ms of darkness. This was done to account for the impacts of the currents that run inside each pixel even when there is no light. Figure 3a shows the response distribution throughout the pixel array when it is irradiated by light with a wavelength of 654 nm, demonstrating that the plasmonic components are rather uniform with the exception of a small number of faulty pixels. Our presented spectrum responses are the average of the responses of all the pixels in the array that share the same plasmonic filter. The performance of the filters has been evaluated by comparing the average response of each pixel design to the average response of the un patterned reference pixels, since measuring the transmission spectrum directly is difficult. In Fig. 3b, we can see the results for pixels equipped with five distinct plasmonic filters, each of which acts as a bandpass filter but has a slightly different center wavelength. Full width at half maximums for these filters range from 110 to 160 nm, but their normalized responses are more than 60% of the signal recorded from an unprocessed pixel. The oscillations in all the answers stand out as a notable aspect of these data that wasn't present in Fig. 1c. We conclude that these oscillations are due to FP resonances in the CIS dielectric stack since they have been detected in both the single pixel plasmonic CMOS photodetector and the responses of pixels prior to any back-end-of-line processing. Resonances are caused by reflections at the interfaces between the dielectric layers due to their varying permittivity's. As commercial CIS often does not make use of a CMOS process that has been optimized to minimize this impact, our finding should come as no surprise.

In Fig. 4, we see the average findings for three sets of pixels whose peak response wavelengths are quite near to the red (700 nm), green (654 nm), and blue (300 nm) standards established by the International Committee on Illumination at 2° in 1931. Information was sent

Figure 4. Three groups of photodiodes with peak responses at 300, 654, and 700 nm were used to generate normalized photocurrents. Similar color glass filters' transmission spectra are shown for evaluation.



It is possible to compare the spectra of the identical filters on glass. By comparing the peak responses of different photodiode pixels to the peak transmission λ_max of the plasmonic

Copyright The Author(s) 2023.This is an Open Access Article distributed under the CC BY license. (http://creativecommons.org/licenses/by/4.0/)

Journal of Image Processing and Intelligent Remote Sensing
ISSN 2815-0953
Vol: 03, No. 03, April-May 2023
http://journal.hmjournals.com/index.php/JIPIRS
DOI: https://doi.org/10.55529/jipirs.33.1.8

color filters on glass, a blue shift is seen for all pixels. The integrated on-chip filters have smaller hole sizes than glass filters, and CMOS devices also experience the highindex substrate loading effect, both of which contribute to this problem. Adjusting the procedure for color matching may get rid of this impact. Also, it seems that CIS-made filters have larger transmission bands than their glass counterparts. A larger variety cross-talk generated by the wide vertical gap, 6 m, between photodiodes underneath and the filters; and variations in angles of incidence of light happening during testing of the pixels; may all play a role in this growth. These considerations suggest that the reported results may not be indicative of those that would be realized in an ideal manufacturing approach, especially if the plasmonic color filters are incorporated in lower metal layers in a standard CMOS process. The use of narrow band filters, such as low loss silver filters, is another method for mitigating the widening effect. These plasmonic nanostructures, when created in close proximity to the photodiodes, the optoelectronic efficiency is enhanced since the localized field is potentially much magnified due to the SPR effects.

2. CONCLUSION

a replacement for the conventional pigment dye filters used in industrial CIS has been offered in the form of a plasmonic color filter integrated into a 150×150-pixel CIS. dry etch and Electron beam lithography were used in the final stages of production to create a functional plasmonic CIS. Photocurrent characterization of photodiode pixels using a variety of plasmonic filters exhibited plasmonic color selectivity. Transmission of the identical filters built on glass agrees well with the normalized photocurrents of the CIS's integrated plasmonic color filter. Understanding the impact of color cross-talk will need further research. This study may help with the design of next-generation CIS that is less expensive, has less cross-talk, and doesn't rely on complex multilayer processing of dye-based filters.

3. REFERENCES

1. Hassan, M. D., Nasret, A. N., Baker, M. R., & Mahmood, Z. S. (2021). Enhancement automatic speech recognition by deep neural networks. Periodicals of Engineering and Natural Sciences, 9(4), 921-927.
2. Mahmood, Z. S., Coran, A. N. N., & Aewayd, A. Y. (2019, October). The impact of relay node deployment in vehicle ad hoc network: Reachability enhancement approach. In 2019 Global Conference for Advancement in Technology (GCAT) (pp. 1-3). IEEE.
3. Mahmood, Z., Nasret, A., & Awed, A. (2019, September). Design of new multiband slot antennas for wi-fi devices. In International Journal on Communications Antenna and Propagation (IRECAP) (Vol. 9, No. 5).
4. Mahmood, Z. S., Nasret, A. N., & Mahmood, O. T. (2021, October). Separately excited DC motor speed using ANN neural network. In AIP Conference Proceedings (Vol. 2404, No. 1, p. 080012). AIP Publishing LLC.
5. Mahmood, Z. S., Coran, A. N. N., esam Kamal, A., & Noori, A. B. (2021, August). Dynamic spectrum sharing is the best way to modify spectrum resources. In 2021 Asian Conference on Innovation in Technology (ASIANCON) (pp. 1-5).
6. Nasret, A., & Mahmood, Z. (2019). Optimization and integration of rfid navigation

Copyright The Author(s) 2023.This is an Open Access Article distributed under the CC BY license. (http://creativecommons.org/licenses/by/4.0/)

Journal of Image Processing and Intelligent Remote Sensing
ISSN 2815-0953
Vol: 03, No. 03, April-May 2023
http://journal.hmjournals.com/index.php/JIPIRS
DOI: https://doi.org/10.55529/jipirs.33.1.8

system by using different location algorithms. International Review of Electrical Engineering (IREE), 14(4).
7. Mahmood, Z. S., Coran, A. N. N., & Kamal, A. E. (2018). Dynamic approach for spectrum sharing in cognitive radio. International Journal of Engineering & Technology, 7(4), 5408-5411.
8. Nasret, A. N., Noori, A. B., Mohammed, A. A., & Mahmood, Z. S. (2021). Design of automatic speech recognition in noisy environments enhancement and modification. Periodicals of Engineering and Natural Sciences, 10(1), 71-77.
9. NASRET, A. N., KAMAL, A. E., & MAHMOOD, Z. S. Radar Target Detection by Using Levenberg-Marquardt Algorithm.
10. Mahmood, Z. S., Kadhim, I. B., & Nasret, A. N. (2021). Design of rotary inverted pendulum swinging-up and stabilizing. Periodicals of Engineering and Natural Sciences, 9(4), 913-920.
11. Coran, A. N. N., Mahmood, Z. S., & Kamal, A. E. (2021, October). Classification of Acoustic Data Using the FF Neural Network and Random Forest Method. In 2021 International Conference on Smart Generation Computing, Communication and Networking (SMART GENCON) (pp. 1-4). IEEE.
12. Coran, A. N. N., Sever, P. D. H., & Amin, D. M. A. M. (2019). Acoustic data classification using random forest algorithm and feed forward neural network. In IEEE global conference for advancement in technology.
13. Laylani, L. A. A. S. S., Coran, A. N. N., & Mahmood, Z. S. (2022, January). Foretelling Diabetic Disease Using a Machine Learning Algorithms. In 2022 International Conference for Advancement in Technology (ICONAT) (pp. 1-5). IEEE.
14. Kamal, A. E., Salih, A. B., & Coran, A. N. N. (2018). Spectrum sensing algorithm using ANN in cognitive radio. International Journal of Engineering & Technology, 7(4), 5151-5155.
15. Kadhim, I. B., Khaleel, M. F., Mahmood, Z. S., & Coran, A. N. N. (2022, August). Reinforcement Learning for Speech Recognition using Recurrent Neural Networks. In 2022 2nd Asian Conference on Innovation in Technology (ASIANCON) (pp. 1-5). IEEE.
16. Kadhim, I. B., Nasret, A. N., & Mahmood, Z. S. (2022). Enhancement and modification of automatic speaker verification by utilizing hidden Markov model. Indonesian Journal of Electrical Engineering and Computer Science, 27(3), 1397-1403.
17. Coran, A. N. N., Ali, A. H. M., Mahhmood, Z. S., & Mohammed, S. F. (2021, December). Design Speech Recognition Systems in the nosily Environment by Utilizing intelligent Devices. In 2021 Second International Conference on Smart Technologies in Computing, Electrical and Electronics (ICSTCEE) (pp. 1-6). IEEE.
18. Coran, A. N. N., Mahmood, Z. S., & Salih, A. B. (2018). Satellite network underlying LMS for coverage and performance enhancement. International Journal of Engineering & Technology, 7(4), 5404-5407.
19. Mezaal, Y. S., & Nasret, A. N. A New Microstrip Bandpass Filter Design Based on Slotted Patch Resonator.
20. Mahmood, Z. S. (2012). YÜKSEK LISANS TEZI.
21. Aaref, A., & Mahmood, Z. (2021). Optimization the accuracy of ffnn based speaker recognition system using pso algorithm. International Journal on Communications Antenna and Propagation (IRECAP), 11(4).

Copyright The Author(s) 2023.This is an Open Access Article distributed under the CC BY license. (http://creativecommons.org/licenses/by/4.0/)